Time-dependent Schrödinger equation method: Application to charge transfer and excitation in H and H^+ collisions

Xiao-Min Tong,[1] Daiji Kato,[1] Tsutomu Watanabe,[2] and Shunsuke Ohtani[1,3]
[1]*Cold Trapped Ions Project, ICORP, JST, Axis 3F, 1-40-2 Fuda Chofu, Tokyo 182-0024, Japan*
[2]*Physics Department, International Christian University, Mitaka, Tokyo 181-8585, Japan*
[3]*Institute for Laser Science, University of Electro-Communication, Chofu, Tokyo 182-0021, Japan*
(Received 15 December 1999; revised manuscript received 8 May 2000; published 10 October 2000)

We have studied the excitation and charge transfer (including resonant charge transfer) processes of H and H^+ collisions in a wide range of collision energies by solving the time-dependent Schrödinger equation with the classical trajectory approximation for the projectile. The time-dependent Schrödinger equation is solved by the split-operator method with a generalized pseudospectral (nonuniform grid) method. The calculated impact excitation and charge transfer cross sections are in reasonable agreement with the available experimental measurements. Such a time-dependent Schrödinger equation method can be used to study atom-ion collisions in a wide range of collision energies. Moreover, the time-dependent Schrödinger equation method can provide more dynamic information and physical insights. Combined with time-dependent density functional theory, our time propagator holds significant promise for many-electron processes in the interactions of highly charged ions with atoms, molecules, and solids.

PACS number(s): 34.70.+e, 34.50.Fa

I. INTRODUCTION

Atom-ion collisions have been a subject of interest for a long time [1,2]. There are many theoretical approaches applied to various processes involved in the collisions in different impact energy regions. The excitation process in atom-ion collisions can be studied by the Born approximation at high energies. The charge transfer process involves an electron rearrangement and is very difficult to study by perturbation methods. So far, the best available theoretical methods are the close-coupling [3,4] and classic trajectory methods [5]. The advantage of the close-coupling method lies in that we can choose physically important configurations as the basis and study the specified process with a reasonable computational effort. The disadvantage of the method is that the computational effort increases dramatically if we want to study many-electron process in atom-ion collisions. With the advance of computer technology, we have almost reached the stage of solving the time-dependent Schrödinger equation numerically to study various processes involved in atom-ion collisions. Nagano *et al.* [6] studied many-electron charge transfer process between highly charged ions and atoms by the time-dependent local density approximation method. Their results are not in good agreement with the experimental measurements. The discrepancies might be due to the time-dependent local density approximation or the numerical approach, which needs further investigation. Recently, Schultz *et al.* [7] calculated the excitation cross section in H and H^+ collisions in a wide range of collision energies by the lattice (equal space mesh) time-dependent method and their results are in reasonable agreement with the available experiments. To investigate the charge transfer process, they suggested that a nonuniform mesh should be used. All these results stimulate us to study atom-ion collisions by solving the time-dependent Schrödinger equation with the split-operator and pseudospectral (nonuniform mesh) method in the energy representation [8]. This method has been successfully applied to studies of high-order harmonic generation in pulsed laser fields [9,10] and high-resolution spectra of Rydberg atoms in external fields [11,12]. With this method, we can study the excitation and charge transfer processes in atom-ion collisions. The purposes of the present work are (1) testing the capability of our time-dependent propagation method in atom-ion collisions; (2) preparing an accurate, efficient time-propagation method for time-dependent density functional theory [9,13], which can be used to study many-electron transfer processes in the collisions of highly charged ions with atoms, molecules, and solids.

As a test example, we have studied the excitation and charge transfer (including resonant charge transfer) processes of H and H^+ collisions in a wide range of collision energies. Our calculated $2s$ and $2p$ excitation cross sections are in good agreement with those of the lattice time-dependent method [7], and $2s$ and $2p$ transfer cross sections in reasonable agreement with the available experiments. We will give a brief description of our theoretical method in Sec. II and present our results and a discussion in Sec. III. After presenting our results, the relation between our grid method and the close-coupling method is discussed.

II. THEORETICAL METHOD

H and H^+ collisions can be studied by solving the time-dependent Schrödinger equation for a given impact parameter b (atomic units with $\hbar = m = e = 1$ are used throughout unless explicitly stated otherwise) as

$$i\frac{\partial}{\partial t}\psi(t) = H(t)\psi(t), \tag{1}$$

with the initial wave function in the target H ground state. If we choose H^+ moving along the z direction and the impact

parameter b along the x direction with a straight line trajectory approximation, the time-dependent Hamiltonian of the system can be expressed as

$$H(t)=-\frac{\nabla^2}{2}-\frac{1}{r}-\frac{1}{|\mathbf{r}-\mathbf{R}(t)|}, \tag{2}$$

with $\mathbf{R}(t)=(b,0,z_0+vt)$. Here z_0 is the initial position of H^+ in the z direction and v is the impact velocity of the projectile. The target H atom is placed at the origin. We recast $H(t)$ as

$$H(t)=H_0+V(t),$$

$$H_0=-\frac{\nabla^2}{2}-\frac{1}{r}, \tag{3}$$

$$V(t)=-\frac{1}{|\mathbf{r}-\mathbf{R}(t)|},$$

and solve Eq. (1) by the second-order split-operator method in the energy representation [8,11] as

$$\psi(t+\Delta t)=e^{-iH_0\Delta t/2}e^{-iV(t)\Delta t}e^{-iH_0\Delta t/2}\psi(t). \tag{4}$$

To propagate the wave function in Eq. (4), we use spherical coordinates and the radial part is discretized by the pseudospectral grid method [14]. The detailed numerical procedure for solving the time-dependent Schrödinger equation can be found in Refs. [8,10,11]. Supposing the projectile leaves the interaction region at $t=T$, the excitation or charge transfer probabilities can be obtained by projecting the final time-dependent wave function onto the state we are interested in as

$$P(t,b)=\begin{cases}|\langle\phi_t|\psi(t)\rangle|^2 & \text{excitation}\\ |\langle\phi_p|\psi(t)\rangle|^2 & \text{transfer,}\end{cases} \tag{5}$$

with ϕ_t,ϕ_p the time-independent wave functions of the target and projectile atoms. Note that, for the time-independent wave function of the projectile, an electron translation factor [3] is included. The corresponding cross section can be obtained from

$$\sigma=2\pi\int_0^\infty P(T,b)bdb. \tag{6}$$

III. RESULTS AND DISCUSSION

As a test example, we have studied $H+H^+$ collisions in a wide range of collision energies (from 1 to 1000 keV). All the calculations are performed in a four PC LINUX cluster with a Pentium III 400 MHz CPU. As illustrated in Sec. II, we use spherical coordinates with $r_{max}=150$ a.u. and 50 partial waves in the calculations. The radial part is discretized in a *nonuniform* pseudospectral grid with 100 grid points. At $t=0$, we put the projectile H^+ at $z_0=-24$ a.u. with the impact parameter b along the x direction. The initial wave function is located in the target H $1s$ state at the origin of the coordinates. The time-dependent wave function is propagated by Eq. (4) with the projectile moving along a straight line from z_0 to $z_T=36$ a.u. One thousand time steps and 20 to 30 impact parameters are used in the calculations.

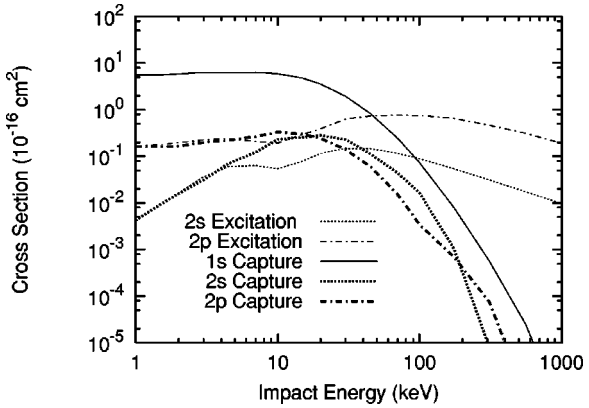

FIG. 1. Excitation and transfer cross sections in $H+H^+$ collisions. Thin dashed line for $2s$ excitation; thin dot-dashed line for $2p$ excitation; thick dashed line for $2s$ capture; thick dot-dashed line for $2p$ capture; thin solid line for resonant charge capture.

To test the numerical stability, we have also performed a calculation at low impact energy (1 keV) by using 200 grid points in the radial part, 60 partial waves, and 3000 time steps. The final results of the two calculations are in good agreement with each other for the total cross section and excitation cross sections (within 1%). The largest error (about 10%) appears in the $2s$ transfer cross section. The unitarity or normalization of the time-dependent wave function is also tested by setting $V(t)=0$ in Eq. (4) and the normalization is accurate to 10 digits. To save computer time and storage space, we output the dynamic probabilities, induced dipole, and normalization every 10 time steps.

A. Excitation and charge transfer processes in H and H^+ collisions

Figure 1 shows general features of the excitation and charge transfer (including resonant charge transfer) cross sections in H and H^+ collisions. The resonant charge transfer is the dominant process in the low-energy region and decreases rapidly as the collision energy increases. At low energies (<10 keV), the $2s$, $2p$ charge transfer cross sections are almost the same as the corresponding excitation cross sections as shown in Fig. 1. The $2p$ excitation and charge transfer cross sections increase smoothly as the energy increases. The $2s$ excitation and transfer cross sections increase rather rapidly in this energy region. As the energy approaches 10 keV, the $2s$ and $2p$ transfer cross sections reach a maximum. The $2s$ and $2p$ excitation cross sections have a dip near 10 keV. As the energy increases further (above 20 keV), the charge transfer cross sections drop very rapidly. Excitation cross sections also decrease as the energy increases at high energies (above 50 keV) as shown in Fig. 1. We will discuss the detailed physical insights from the observations later. Now, let us first compare the electron excitation and transfer cross sections with experiments.

Figure 2 shows the $2s$ and $2p$ excitation cross sections. Our calculated $2s$ excitation cross sections are in good

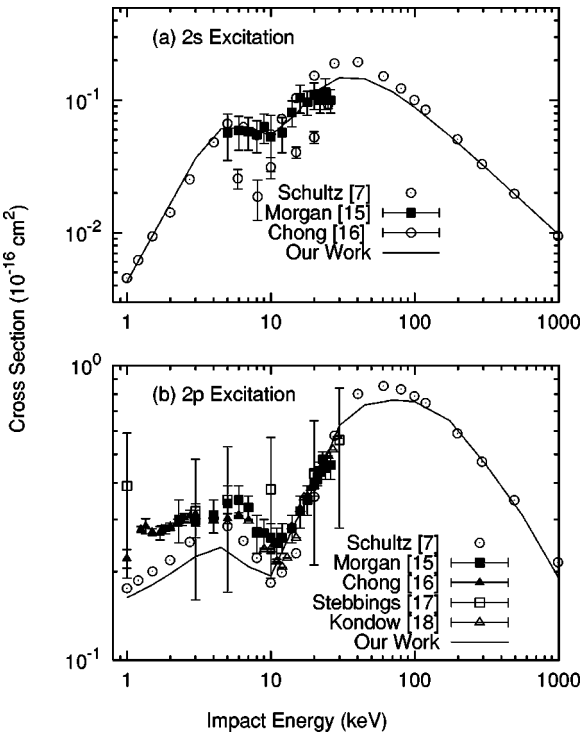

FIG. 2. Excitation cross sections for (a) $2s$ and (b) $2p$ in $H+H^+$ collisions.

agreement with the recent lattice time-dependent results [7] (open circles) at both the low- and high-energy ends as shown in Fig. 2(a). Discrepancies between the two calculations of $2s$ excitation appear near the peak position (30 keV). Both theoretical results are in reasonable agreement with the experiment [15]. The experimental data from Ref. [16] are significantly lower than the theoretical values. For $2p$ excitation, our results are lower than those of Ref. [7] at low energies and those results are closer to the experimental measurements [17,18]. Near the peak position (50 keV), as in $2s$ excitation, our calculated $2p$ excitation cross section is lower than that of Ref. [7]. Since Schultz *et al.* [7] have already compared their excitation cross sections with the experimental data extensively, we will focus on the charge transfer process, which was not studied in Ref. [7].

Figure 3 shows the resonant capture cross section in $H+H^+$ collisions. Since $1s$ is a tightly bound state, resonant capture is the most challenging process for numerical calculations. Based on the grid parameter given above, we project the analytical $1s$ wave function of the projectile into the numerical grid and the normalization of the wave function has 10% error when the projectile is farthest from the target. The resonant capture cross section changes very smoothly at low energies (below 10 keV) and decreases rapidly when the collision energy increases above 10 keV. Our calculated resonant capture cross sections are in good agreement with other theoretical results [19,20] as shown in Fig. 3.

Figure 4 shows the $2s$ and $2p$ transfer cross sections. Our calculated $2s$ and $2p$ charge transfer cross sections are in agreement with other theoretical results [19,21] as shown in Fig. 4. For $2s$ transfer, our results are in good agreement with the experimental measurements [15,16,22–24] when

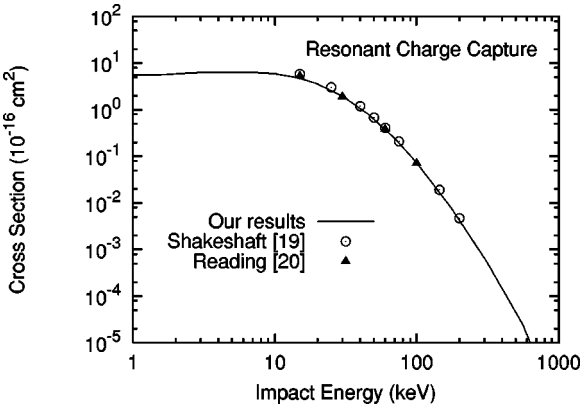

FIG. 3. Resonant charge capture cross sections in $H(1s)+H^+ \rightarrow H^+ + H(1s)$ collisions.

the collision energy is above 5 keV. Large discrepancies appear at lower energies (below 5 keV). This implies that further experimental as well as theoretical studies are needed at low energies. The $2s$ transfer cross section first increases as the energy increases, reaches a maximum near 20 keV, and then decreases dramatically as the energy increases further. Unlike the $2s$ case, the $2p$ transfer cross section increases smoothly from 1 keV to 10 keV, and then decreases as the energy increases further. Our calculated $2p$ transfer cross section is in reasonable agreement with the experimental measurements [15,17,18].

B. Dynamic excitation and transfer probabilities

Figure 5 shows the dynamic $2p_x$ excitation and charge transfer probabilities $P(t,b)$ defined in Eq. (5) with collision

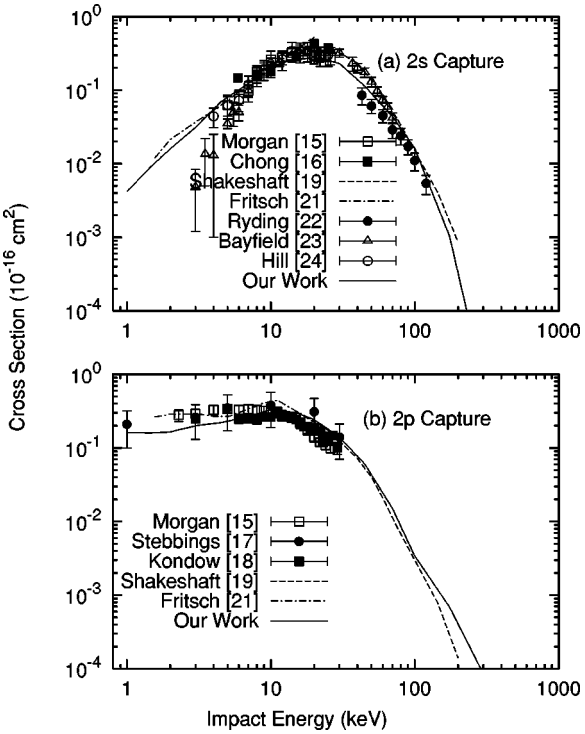

FIG. 4. Charge transfer cross sections for (a) $2s$ and (b) $2p$ in $H+H^+$ collisions.

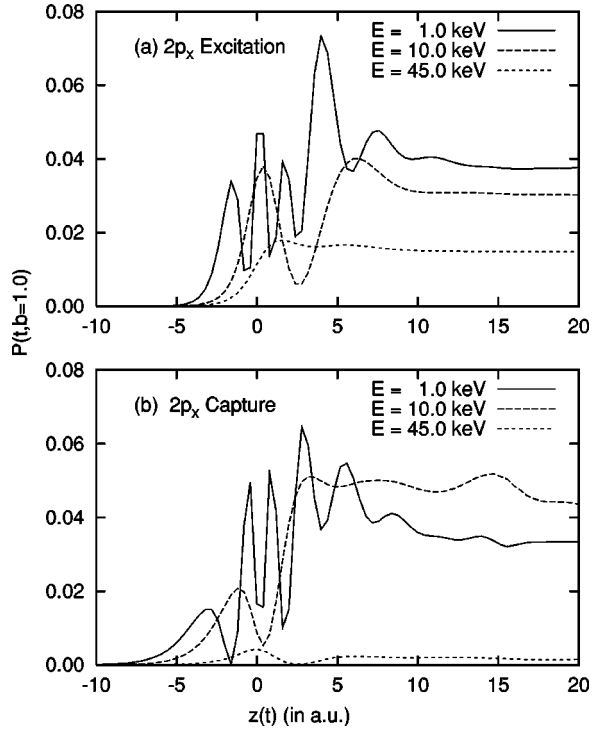

FIG. 5. The dynamic probabilities of (a) $2p_x$ excitation and (b) $2p_x$ transfer with impact parameter $b=1.0$ a.u.

energies of 1.0, 10.0, and 45.0 keV, respectively, and impact parameter $b=1.0$ a.u. Let us first study the excitation process. At low energy, the excitation probability oscillates very rapidly when the projectile is near the target atom as shown in Fig. 5(a). As the energy increases to 10 keV, the probability oscillates once and reaches asymptotic behavior. As the energy increases further to 45.0 keV, the probability increases monotonically and reaches a plateau. The oscillation of the probabilities represents a rearrangement of the electron in the collision process and a monotonic increase represents direct field excitation as we explained above. Due to the effect of Stuckelberg-type scattering, the oscillations also appear in the $2p_x$ transfer probability. As the energy increases, the duration time of the projectile near the target atom is shorter and the electron wave packet cannot move back and forth between the two nuclei. So the rearrangement contribution to the excitation or charge transfer gets smaller as the interaction time gets shorter for higher impact energy. When the two nuclei are far from each other, the dynamic probabilities represent the excitation or charge transfer probabilities. When the two nuclei are close to each other, it is very difficult to distinguish whether the electron is bound to the target or projectile since the target wave function greatly overlaps the projectile wave function, but the physical information represented by the dynamic probabilities is still qualitatively correct.

After presenting our numerical results and discussion, it it very interesting to compare our procedure with the close-coupling method [3] from a more fundamental point of view. In the close-coupling method, we have to choose a basis of orbitals. Such orbitals could be one-atomic-center orbitals [25], two-atomic-center orbitals [26–28], or molecular orbitals [29,30]. The choice of the basis of orbitals depends on the physical process we are interested in, computational effort, convergence, and so on. If we could include a complete basis set of the orbitals, we could study a collision process with any kind of basis. In practice, it is very difficult to include a complete basis set although we can include a very large basis set as discussed in Ref. [31]. In our time-dependent method we use the grid method instead of a basis set. Such a grid structure has a relation to one atomic orbital when we propagate the wave function in the energy representation as shown in Eq. (4). Since our one atomic orbital forms a ''complete'' basis set and we do not need to calculate the overlap and the interaction matrix in the time propagation, our method is more efficient than the close-coupling method. The completeness of the basis set or optimized grid structure is checked by the description of the projectile and target wave functions in the grid structure when they are far away from each other. All these have been checked in our grid method calculation. If we convert the parameters used in our calculation into the number of one-atomic orbitals, we have used 100 orbitals in each partial wave and 50 partial waves with all possible magnetic quantum numbers. Thus the total number of orbitals is 250 000. The other advantage of the grid method is that we can extend the numerical method to study many-electron processes by the time-dependent density functional method [9].

To summarize, we have presented a theoretical study of H and H^+ collisions by solving the time-dependent Schrödinger equation. The calculated excitation and charge transfer cross sections are in reasonable agreement with the available experiments. Such studies can provide useful physical insights into the collision processes at a wide range of collision energies. Therefore, combined with the time-dependent density functional theory, our time-dependent Schrödinger method holds significant promise for understanding many-electron processes in the interactions of highly charged ions with atoms, molecules, and solids.

ACKNOWLEDGMENTS

The experimental data were obtained by use of the numerical atomic and molecular data bases at the National Institute for Fusion Science (NIFS), Japan.

[1] B.H. Bransden and M.R.C. McDowell, *Charge Exchange and the Theory of Ion-Atom Collisions* (Clarendon Press, New York, 1992).

[2] C.D. Lin, *Review of Fundamental Processes and Application of Atoms and Ions* (World Scientific, Singapore, 1993).

[3] W. Fritsch and C.D. Lin, Phys. Rep. **202**, 1 (1991).

[4] N. Toshima, Phys. Rev. A **50**, 3940 (1994).

[5] C. Illescas and A. Riera, Phys. Rev. A **60**, 4546 (1999).

[6] R. Nagano, K. Yabana, T. Tazawa, and Y. Abe, J. Phys. B **32**, L65 (1999).

[7] D.R. Schultz, M.R. Staryer, and J.C. Wells, Phys. Rev. Lett. **82**, 3976 (1999).
[8] X.M. Tong and S.I. Chu, Chem. Phys. **217**, 119 (1997).
[9] X.M. Tong and S.I. Chu, Phys. Rev. A **57**, 452 (1998).
[10] X.M. Tong and S.I. Chu, Phys. Rev. A **58**, R2656 (1998).
[11] S.-I. Chu and X.M. Tong, Chem. Phys. Lett. **294**, 31 (1998).
[12] X.M. Tong and S.I. Chu, Phys. Rev. A **61**, 031401R (2000).
[13] X.M. Tong and S.I. Chu, Int. J. Quantum Chem. **69**, 293 (1998).
[14] G. Yao and S.I. Chu, Chem. Phys. Lett. **204**, 381 (1993).
[15] T.F. Morgan, J. Geddes, and H.B. Gilbody, J. Phys. B **6**, 2118 (1973).
[16] Y.P. Chong and W.L. Fite, Phys. Rev. A **16**, 933 (1977).
[17] R.F. Stebbings, R.A. Young, C.L. Oxley, and H. Everhardt, Phys. Rev. **138**, A1312 (1965).
[18] T. Kondow, R.J. Girnius, Y. Chang, and W.L. Fite, Phys. Rev. A **10**, 1167 (1974).
[19] R. Shakeshaft, Phys. Rev. A **18**, 1930 (1978).
[20] J.F. Reading, A.L. Ford, and R.L. Becker, J. Phys. B **14**, 1995 (1981).
[21] W. Fritsch and C.D. Lin, Phys. Rev. A **26**, 762 (1982).
[22] G. Ryding, A.B. Wittkower, and H.B. Gilbody, Proc. Phys. Soc. London **89**, 547 (1966).
[23] J.E. Bayfield, Phys. Rev. **185**, 105 (1969).
[24] J. Hill, J. Geddes, and H.B. Gilbody, J. Phys. B **12**, L341 (1979).
[25] K.A. Hall, J.F. Reading, and A.L. Ford, J. Phys. B **29**, 6123 (1996).
[26] J. Kuang and C.D. Lin, J. Phys. B **29**, 1207 (1996).
[27] H.A. Slim and A.M. Ermolaev, J. Phys. B **27**, L203 (1994).
[28] N. Toshima, J. Phys. B **30**, L131 (1997).
[29] C. Harel *et al.*, Phys. Rev. A **55**, 287 (1997).
[30] L.F. Errea *et al.*, J. Phys. B **31**, 3199 (1998).
[31] J. Kuang and C. Lin, J. Phys. B **30**, 101 (1997).